Mechanical Properties of 1,2,4,5-Benzene Tetra Carboxylic Chitosan-Filled Chitosan Biocomposites

Nurhidayatullaili Muhd Julkapli, Zulkifli Ahmad, Hazizan Md Akil

School of Material and Mineral Resources Engineering, Universiti Sains Malaysia, 11300 Seberang Perai Selatan, Pulau Pinang, Malaysia

Received 11 February 2010; accepted 7 September 2010
DOI 10.1002/app.33393
Published online 16 February 2011 in Wiley Online Library (wileyonlinelibrary.com).

ABSTRACT: The degree of matrix-filler interaction plays an important role in determining the mechanical properties of biocomposite materials. To produce highly compatible chitosan biocomposites, 1,2,4,5-benzene tetra carboxylic chitosan (BTC) was used as a filler to reinforce a chitosan matrix (Cs), because the similar backbone structure of Cs and BTC filler is expected to increase the compatibility of the biocomposite. The mechanical properties of these biocomposites were investigated under tension and tearing mode. Introduction of BTC filler (at 0, 2, 4, 6, 8, and 10 wt%) provided dramatic increments in σ_R and E values, but the observed values of ε_R and K correlated negatively to similar levels of BTC filler. Morphological results demonstrate that the breaking surfaces of biocomposites form rugged deformation lines, resulting in high σ_K values of the biocomposites. © 2011 Wiley Periodicals, Inc. J Appl Polym Sci 121: 111–126, 2011

Key words: chitosan; biocompatibility; mechanical properties; biocomposites; crosslinking

INTRODUCTION

Researchers and industrialists are expressing a wide revival of interest in the utilization of oil-based biodegradable plastics (DP) for packaging, a niche in which nondegradable plastics have traditionally been the materials of choice.[1–3] Although brittleness and uncontrolled degradation rate of oil-based DP[4,5] have presented a problem for their use in packaging, the introduction of 30–50% of natural polymer such as cellulose and starch has been found able to overcome the problem,[6–8] but at the price of scarifying most of its mechanical properties. Alternatively, DP from vegetable crops could be the solution[9] for use in packaging applications with its combination of properties: lightweight, with good resistance, relatively low cost, and completely degradable in a compost facility. However, the production of this material competes with the production of food. It has been estimated that 1.62 m^2 of farmland are needed to produce a single kilogram of this material.

Therefore, biowaste-based DP has been recently been used to replace the oil-based and vegetable-based DP to limit the problem of degradability and the cost of production. Chitosan (Cs), which consists of glucosamine and acetylglucoseamnie copolymers,[10] is one of the main biowaste-based DP.[10] Cs is produced commercially by deacetylation of chitin, the structural element in the exoskeleton of crustaceans (crabs, shrimps) and cell wall of fungi.[11] Therefore, Cs can be considered economical, readily available, biodegradable, and highly safe. Recent research has sought to incorporate the Cs materials with the reinforcement filler to enhance the composite's mechanical properties while limiting its brittleness[12–24] (Table I).

Although the reinforcement approach is evidently able to increase the mechanical properties of Cs materials,[12–24] compatibility between the incorporated components of such composites is still poor. It is believed that use of more compatible filler in the Cs matrix will further improve its properties. Therefore, in this study, the crosslinked chitosan filler (CCF) was introduced as a reinforcement agent for the Cs system. CCF exhibits superior qualities such as thermal stability, high glass transition temperature, low shrinkage at elevated temperature and resistance to most chemicals, and solvents.[25,26] Indeed, the potential use of CCF is greatly enhanced by their hydrophilic character, which leads to good interfacial bonding with the polar groups of Cs. Consequently, 1,2,4,5-benzene tetra carboxylic chitosan (BTC) (Fig. 1) was used in this study as the CCF material for reinforcement of the structure of Cs. The effects of the compatibility and homogeneity of this combination were evaluated through characterization of the composite's mechanical properties (under tensile and tearing mode), analysis of the chemical interaction between such components

Correspondence to: H. M. Akil (hazizan@eng.usm.my).

TABLE I
Mechanical Properties of Chitosan Composites with Respect of Different Types of Filler

Types of samples	Tensile strength (MPa)	Elongation at break (%)	Young Modulus (MPa)	References
2% Chitosan film	39.47 ± 6.6	37.44 ± 2.9	–	12
2% Chitosan + 0.3% PEG	14.57 ± 1.7	49.56 ± 3.1	–	12
2% Chitosan + 0.3% sorbiol	38.48 ± 3.3	56.91 ± 4.2	–	12
2% Chitosan + 0.6% glycerol	33.69 ± 3.7	167 ± 3.6	–	12
Chitosan + collagen	1.19 ± 0.4	–	39.78 ± 5.60	13
Chitosan + collagen + HA	21.88 ± 3.21	–	1159.5 ± 79.1	13
Chitosan + 30 wt% CMC	3.5	–	–	14
Chitosan film	75	2.6	5000	15
Chitosan + 1 wt% BC	110	2.8	7000	15
2% chitosan film	82 ± 15	4 ± 3.2	–	16
2% chitosan + 3 w/w% MNC	60 ± 10	6 ± 0.5	–	16
Chitosan film	39.6 ± 3.2	15.2 ± 1.2	200.1 ± 0.12	17
Chitosan + 0.2% MWCNTs	102.8 ± 3.6	7.9 ± 1.1	435 ± 0.26	17
Chitosan film	85	20	–	18
Chitosan + 20 wt% CW	120	6	–	18
Chitosan film	12	17	310	19
Chitosan + 1 v/w% OA	18	15	495	19
Chitosan film	2	62	–	20
Chitosan + 25% PCL	6.2	35	–	20
Chitosan film	25.99 ± 2.97	28.15 ± 6.15	–	21
Chitosan + 90% v PCL	24.75 ± 4.01	28.69 ± 4.32	–	21
Chitosan film	27	32	–	22
50% Chitosan + 50% starch	40	52	–	22
Chitosan film	62	11.8	–	23
Chitosan + 2.95 wt% αCW	80	8	–	23
Chitosan film	–	4	3000	24
25% Chitosan + 75% MC	–	8	1600	24

PEG, polyethylene glycol; HA, hydroapatite; CMC, carboxylmethyl cellulose; BC, bamboo charcoal; MNC, micro/nano clay; MWCNTs, multiwall carbon nano tube; CW, cellulose whiskers; OA, oleic acid; PCL, polycaprolactone; α-CW, α-chitin whisker; MC, methyl cellulose.

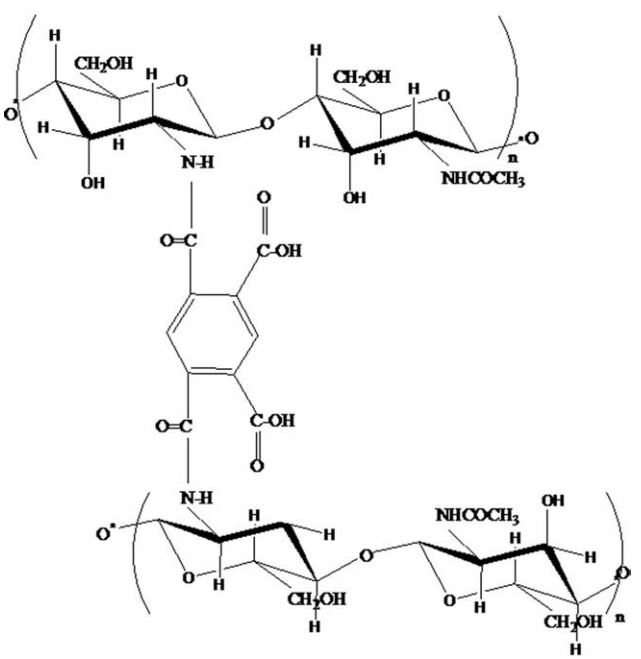

Figure 1 The chemical structure of BTC filler.

[under Fourier Transform Infra red (FTIR) analysis], and the morphology of the fracture surface due to the tensile and tearing test (under FESEM analysis).

MATERIALS AND METHODOLOGY

Raw materials

Cs powder (DD = 60%; Mw = 1300 kD) was purchased from Hunza Pharmaceutical Sdn Bhd (Malaysia). The other ingredients used to prepare biocomposite films were acetic acid (0.1*M*); distilled water; NH_4OH (97% purified); and ethanol.

Preparation of BTC filler

Preparation of BTC filler followed the method described in.[26] In short, Cs structure was crosslinked with 1,2,4,5-benzene tetra carboxylic (as crosslinking agents) in the weight ratio of 2 : 1. The crosslinking reaction was carried out in a nitrogen environment at 150°C for 6 h. The crosslinked product was then filtered, washed, dried, and ground into microscale particles.

TABLE II
Details Composition of BTC-Filled Chitosan Biocomposites

	Parameter		
Composition of BTC filler (%)	BTC filler (g)	Chitosan (g)	0.1 M acetic acid (ml)
0	0	2	100
2	2	2	100
4	4	2	100
6	6	2	100
8	8	2	100
10	10	2	100
12	12	2	100
14	14	2	100

Preparation of BTC-filled chitosan biocomposite films

The film-forming mixture was prepared in several steps. First, BTC filler (at different levels ranging from 2 to 14 wt%) (Table II) mixed in acetic acid solution (95 mL; 0.1*M*). The components were mixed using a magnetic stirrer (20 rpm for 2 h at 35°C) until completely homogenous (with no floating BTC filler). In the second step, Cs powder (2.0 g in the dried form) was added and mixed continuously using a magnetic stirrer (50 rpm for 12 h at 35°C). Distilled water (≈5 mL) was added slowly during the mixing process to obtain 100 mL of film-forming mixture.

The mixture was heated at 40°C and then vigorously mixed for 10 min to improve the dissolving of the Cs powder in the acidic medium. The film-forming mixture was then spread onto a polyethyelene plate (100 mm × 100 mm × 1 mm) and dried at 35°C for 48 h at normal environment.

Finally, the biocomposite films were produced with a film thickness of ~ 0.5 to 0.7 mm. Each produced film was soaked for 30 min at 35° in absolute ethanol containing 0.6 wt% concentrated NH_4OH solution to neutralize the remaining acetic acid.

FTIR analysis

Chemical analysis was done by scanning 10 times with FTIR (Perkin–Elmer, Model: Spectrum One) with a spectrometer in the range of 400 to 4000 cm^{-1}.

Mechanical testing

A tensile test was carried out using a stable universal testing machine (Instron Model 1122) in accordance with the ASTM D 638 standard method. A sample of 100 mm length was clamped into the two jaws of the machine. Each jaw covered 20 mm of the sample. Thus, tensile strength was studied over the rest of 60 mm gauze length. Reading of the tensile strength test instrument for Newton force extension was initially zero. The test was conducted at a constant strain rate of 30 mm/min for 10 sample replicates. Tensile stress was applied till the failure of the sample and the load-extension curve was obtained. The force (N) and deformation at break (in mm) values were used to calculate the tensile strength (Pa) and elongation at break (as %).

A tearing test was performed in accordance with ASTM D-1004 using a universal testing machine (Instron Model 1122) at the high speed of 30 mm/min. The biocomposite films were cut in D-shaped dimensions in accordance with ASTM-1221. The D shape allows the specimen to have an edge cut in the middle of the sample to form two arms, which were then torn apart during the tearing test. A universal testing machine (Instron Model 1122) was used to determine the maximum force (N) and deformation (mm) of the tearing sample.

Morphological observation

The microstructure of the film was evaluated using Field Emission Scanning Electron Microscopy (FESEM, Model Zeiss Supra 35 VP). Before FESEM scanning, the biocomposite films were rinsed in 95% ethanol solution at 20°C for 12 h. The excitation energy used was 5 keV. To achieve good electrical conductivity all samples were first carbon sputtered, followed by sputtering with a gold palladium mixture before examination.

RESULTS AND DISCUSSION

Sample preparation

The homogeneity and uniformity of filler distribution are two main factors that must be clarified and applied to produce BTC-filled chitosan biocomposites with good interfacial bonding. Therefore, homogeneity was applied by dispersing the BTC filler [with relatively 15–80 μm (Fig. 2)] in certain proportions (Table II) in acetic solution under continuous mixing. It was expected that the BTC filler could be mixed into the acidic medium without precipitation, agglomeration and phase separation, yielding a homogenous composite mixture. However, this expectation was not met because of the insolubility properties of the BTC filler in the acidic medium. The BTC filler lacks sufficient NH_2 groups to carry the protonozation[27] process, consequently limiting interhydrogen bonding within the BTC filler. Still, a progressive and continuous mixing process gives the BTC filler the possibility of being present as single particulates in the acidic medium.

Cs powder was then carefully added into the homogenous mixture of BTC filler. The electrostatic interaction and interhydrogen bonding[28] between

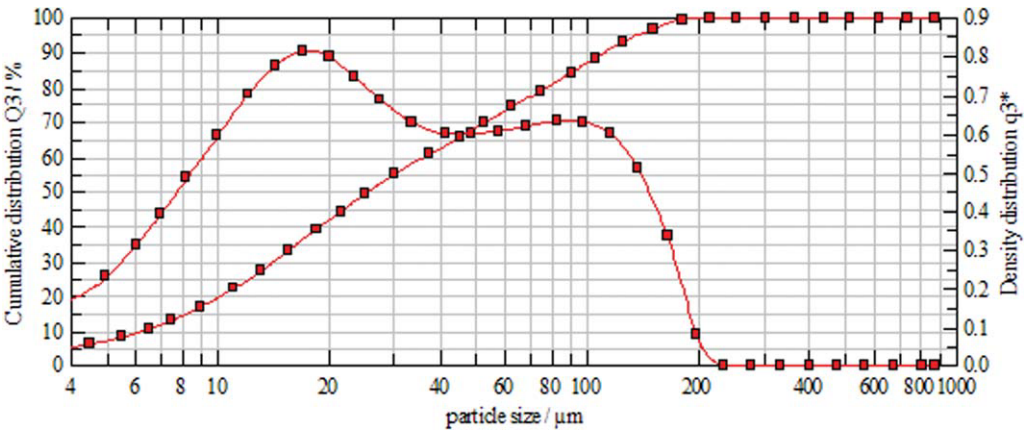

Figure 2 Particle size analysis of BTC filler. The BTC filler was categorized in range size of (4 to 100μm). [Color figure can be viewed in the online issue, which is available at wileyonlinelibrary.com.]

the composite components was simultaneously established after the protonization of NH_2 groups in the Cs matrix.[29,30] Heating aided in the establishment of a greater number of interactions[31] and led to more intense BTC filler-Cs matrix interaction during the drying process.[33–35] The neutralization of NH_3^+ ions was necessary to neutralize the acidic properties of the biocomposite films. The neutralization process was done as accordance to the previous studies.[36–40] Finally, drying time is essential for ensuring that the biocomposite film is completely dried since the presence of water molecules can break down the established interhydrogen bonding of the composite components, inducing a plasticizing effect.

FTIR analysis

Figure 3 shows the infrared spectra changes of BTC-chitosan films at different levels of filler loading (0 to 14 wt/v%). In the infrared measurement of chitosan, the assignments of representative adsorption peaks were identified for all samples: 4000 to 3500 cm^{-1} (hydroxyl); 3840 to 3440 cm^{-1} (secondary amine), 3260 to 3270 cm^{-1} (C—H stretching); 1650 cm^{-1} (primary amide); 1560 cm^{-1} (secondary amide); 1310 cm^{-1} (ternary amide); 1454 cm^{-1} (C-O stretching); and 897 cm^{-1} (β-D-configuration).[26–30] The glucose units of chitosan polymer were completely protected from obliteration during the preparation process of the biocomposite film as indicated by the insignificant change in the adsorption peaks of 1454 cm^{-1} and 897 cm^{-1} for all samples. However, the formation of C = O and C—O in the BTC structure was clearly detected in the adsorption peak at 781 cm^{-1} for the former and a shoulder peak at 1716 cm^{-1} for the latter. Both peaks became more significant for composite samples with 8 to 10 wt/v% of BTC filler.

The adsorption intensity of OH vibration (3000 cm^{-1}) slightly increased (2 to 6%) with the introduction of the BTC filler. The increment values were calculated relatively since the normalization approach is not suitable for application in the composite systems. Such increments indicates the formation of interhydrogen bonding between the composite components.[41–43] The formation of interhydrogen bonding was associated with the NH_2 and NH-R groups. The NH_2 groups of the Cs matrix readily formed interhydrogen bonding with OH and NH-R groups of BTC filler after being protonized in the acidic medium. The polar forces arising from the nature of the biocomposite components aid to form the bonding. The adsorption peaks of NH-R (1650 cm^{-1}) strengthened and blue-shifted to 1664 cm^{-1} with the addition of 2 to 10 wt/v% of BTC filler. However, as the composition of BTC filler rose to 12 wt/v%, the adsorption peak at 1596 cm^{-1} increased in significance. At this point, the excess amounts of BTC filler hindered the NH_2 groups of Cs matrix, reducing the possibility of forming interhydrogen bonding between biocomposite components. It was very difficult to specify which of the functional groups were actually responsible for the interaction. However, the Beer Lambert Law lets it be deduced that any change in adsorption intensity and location of wave length in IR spectrum was mainly due to the formation of hydrogen bonds as long as the thickness of the sample is controlled.[45–47] A number of works have reported that formation of hydrogen bonding affects the intensity and shape of the IR spectrum.[48–50]

The electrostatic interaction of composite components occurred as the COO^- anion was formed from the dissociation of protons from free COOH groups of the BTC filler with positively charged NH_3^+ ions from the conjugated base of the Cs matrix. The formation of H^+ ions as sub product of the dissociation favors heavily the conjugate NH_3^+ structure while the resonance stabilization of the COO^- anion occurred via the adjustment of the aromatic ring.

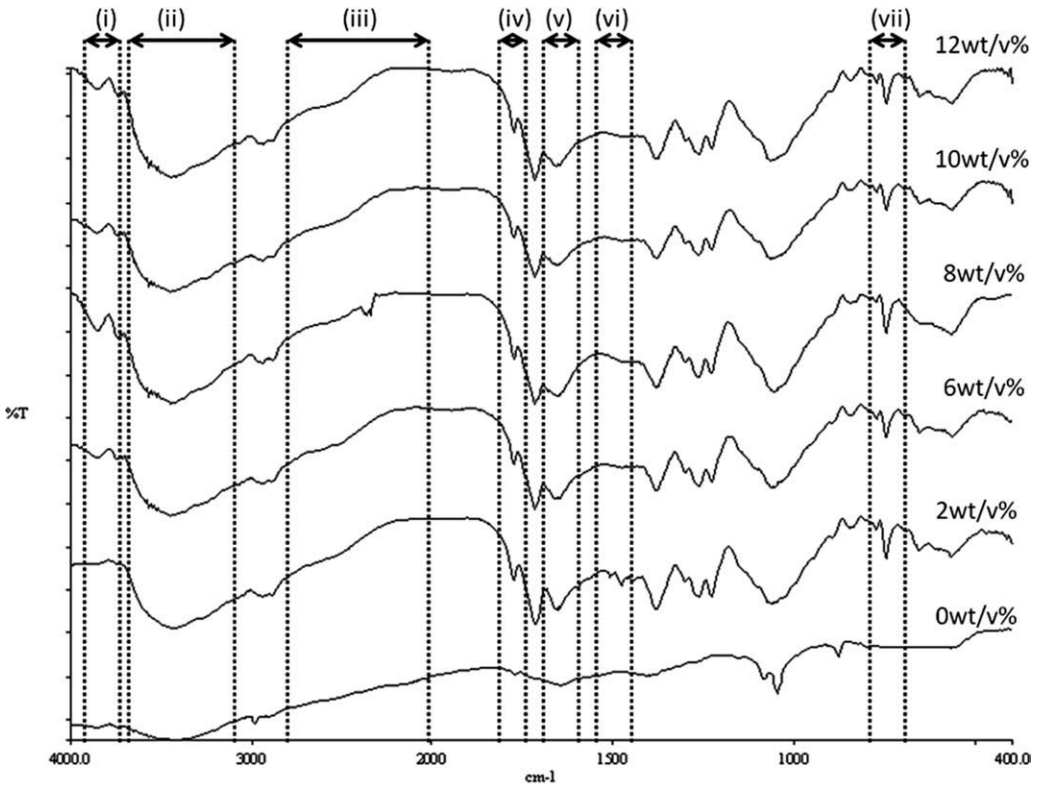

Symbol	Wavenumber (cm^{-1})	Assigments
(i)	3400 -3500	OH and R-NH_2
(ii)	3260-3270	C-H strecthing
(iii)	3000-2000	No significant peak present
(iv)	1716 -1765	C=O to OH ; C=O to C ; C-O
(v)	1664-1650	C=O to NH
(vi)	1596	R-NH-R
(vii)	781	C=O

Figure 3 Series of FTIR spectrum of biocomposites with different of BTC filler loading (0 wt/v%; 2 wt/v%, 6 wt/v%; 8wt/v%; 10 wt/v%; and 12 wt/v%).

The formation of the COO^- anion optimized as the temperature during sample preparation rose to 40°C.

Mechanical properties

Tensile test analysis

Overall, the stress versus strain curve of all examined samples assumed a sigmoid shape similar to that of elastomeric materials, demonstrating a good balance of tensile strength (σ_K) and tensile strain (ε_R), because the linearity relationship of stress over strain was recorded at a certain level after which a nonlinear relationship set in (Fig. 4). As shown in Figure 5, the σ_R values of the biocomposite films increased from 10.76 to 32.93% as BTC filler at 2 to 10 wt/v%, respectively, were introduced into the Cs matrix. Consequently, the elastic modulus (E) values also increased linearly from 11.42 to 30.82%. Meanwhile, the ε_R values were recorded to decrease to 5.56 to 58.62%, followed by a decrease of 4.27 to 62.44% in toughness (K) values. However, as the amount of BTC filler increased to 12 to 14 wt/v%, the σ_R and E values were slightly reduced, to 8.05 to 28.30%, of the values of the parent Cs film. In contrast, ε_R values of the biocomposite films showed positive increments from 3.49 to 18.63% of recorded values.

The progressive improvement in σ_R values indicates a strong interfacial interaction between the composite components, which can be attributed to three main factors. Firstly, BTC filler is expected to give adequate reinforcement effect to the biocomposites films, because it is considered a rigid filler. The rigidity of filler used plays an important role in strengthening composite materials by providing an effective transfer of force (stress) between filler and matrix.[51,52] The crosslinked structure of the BTC filler provides it with a high strength and low extension properties. An adequate level of energy is needed to destroy the whole structure of the BTC filler.[53] At the levels of BTC filler used in this study, introduced energy was adsorbed effectively into the structure of the BTC filler. The adsorption of the

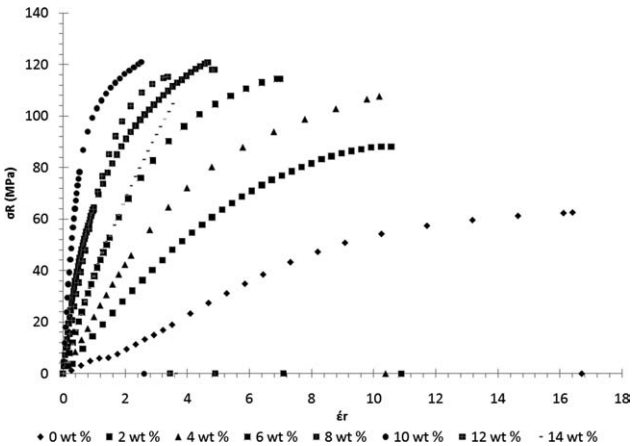

Figure 4 Stress (σ_R) and elongation at break (ε_R) curves of BTC filled chitosan biocomposites at different percentage of BTC filler loading.

energy was balanced by the formation of the cracking mechanism[54] (as indicated by FESEM analysis). The rigid properties of the BTC filler would facilitate in limiting and stopping propagation of cracks, protecting the whole structure of the biocomposite from failure. Therefore, the reinforcement effect was clearly observed in the biocomposites with the higher BTC filler loadings since crack propagation was significantly controlled and limited.

The second factor was attributed to the similarity of the backbone structure of the composite components. Both constituent components are structured with glucosamine as base of their backbone structures, consisting of OH, NH_2 and NH-R as the main functional groups. These groups were responsible for the formation of hydrogen bonds and electrostatic interaction between the biocomposite components. Therefore, increasing in the amount of BTC filler loading linearly increased the number of these interactions and achieved better interfacial bonding.[55] Additionally, an easier attachment and process of incorporation of the BTC filler into the Cs matrix was expected to take place. The BTC filler particles automatically interacted and lodged themselves onto the Cs matrix, which requires only normal conditions (at room temperature) for curing. This consequently produced biocomposite films with better compatibility and high interfacial shear strength.[56] Within the long chain of the Cs molecules bonding is by covalent bond (through β-glycosidic linkage). These primary chemical bonds are of high stability and strength.[57] Therefore, rupture of the bonds within the molecule requires a large amount of energy. Interactions with neighboring molecules in the Cs molecules in a Cs network involve significantly weaker forces. Consequently, a failure of the Cs network is more likely to be due to separation from neighboring molecules rather than to rupture among the Cs molecules.[58]

Finally, the increment of σ_K values of the biocomposite is attributable to the small size of BTC filler particles (Fig. 2), which serve as counter ions and ligands for the BTC filler itself, resulting in increased quality of interfacial bonding of the Cs matrix to the BTC filler. The high surface area of the BTC filler may lead to its stronger dispersion mechanism in the mixture of biocomposites.[59] Each BTC filler particle was expected to form its own individual interface with the Cs matrix. At this point, the probability of forming interactions between the BTC filler particles themselves are significantly reduced. However, the BTC filler is expected to have a greater likelihood of reacting with the Cs matrix during the mixing process, creating finally a greater number of interactions.

However, the addition of BTC at the excess level (12 to 14 wt/v%) reduced slightly the σ_R values of the produced biocomposite films. The reduction indicates a poor adhesion of the interfacial area of the Cs matrix to the BTC filler. At this point, the mode of interaction between the biocomposite components were predominantly changes to inter

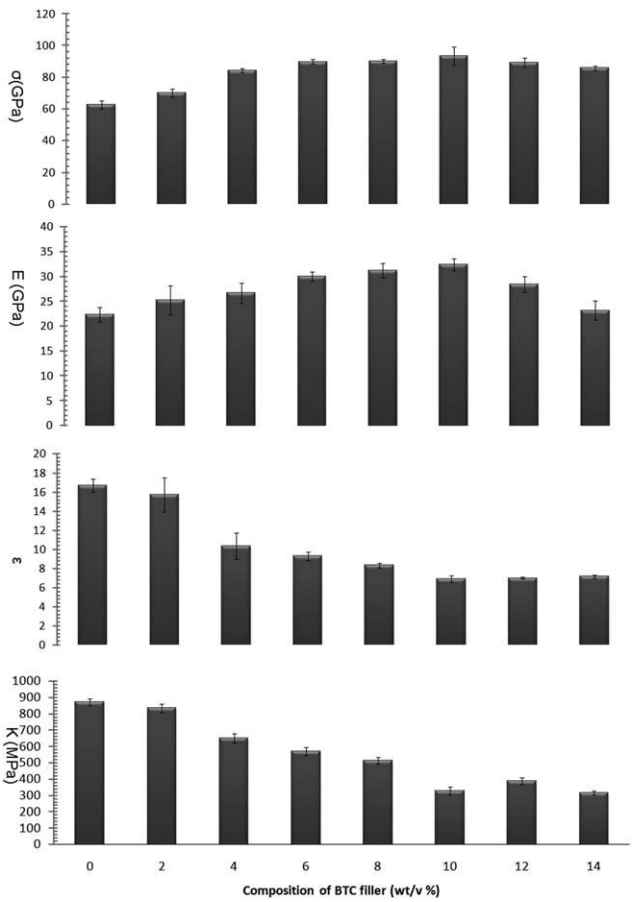

Figure 5 Variation of tensile strength (σ_R); elongation at break (ε_R); Young's Modulus (E) and toughness (K) of the BTC filled chitosan biocomposites at various percentage of BTC filler loading.

molecular interaction rather than to intramolecular interaction. Most presented interactions were achieved between the particles of the BTC filler itself rather than with the Cs matrix. Consequently, the BTC filler was expected to exist as a complex of accumulated particles rather in single particle form. As the content of the Cs matrix of all produced biocomposites was maintained at the same amount, the addition of BTC filler at excess levels would produce biocomposite mixtures with inappropriate filler distribution. Additionally, this nonhomogeneity of the film-forming mixture presents some difficulties for producing biocomposite film with homogenous thickness and appearance. If relatively large agglomerates of BTC filler remain in the Cs matrix, a propagating crack encounters a stress concentration locally, inducing the initiation of failure associated with the weaker intermolecular forces between BTC filler and Cs matrix.[60] At this point, the BTC filler acts as an ineffective reinforcing agent. As a load (stress) is applied, the ineffective reinforcement would take effect along the BTC filler where no stress is carried. The applied stress is not effectively transferred from the Cs matrix to the stronger filler (BTC filler). Shear lag, the mechanism by which stress is transferred along the ends of the agglomerate BTC filler and through the Cs matrix, automatically takes place.[61] A gradual build-up of stress strain along the BTC filler was created up to the maximum or plateau region. This gradual build-up of stress occurs due to the imperfect bonding across the end of the BTC filler. The gradual built-up stress strain also reduces the effective stiffening capacity of the BTC filler.[62] Consequently, the applied stress occurred locally in the Cs matrix before encountering the interfacial area of the biocomposite components. In short, the loss of adhesion between the involved components effectively significantly increased, making the whole structure of biocomposite materials fail prematurely at the lower applied force.

Another factor that contributed to the reduction of σ_R values due to the addition of BTC filler beyond 10 wt/v% was associated with the number of free NH_2 groups in the biocomposite system. As mentioned, formation of inter- and intrahydrogen bonding strongly influenced the mechanical properties of the produced biocomposite film. The NH_2 groups of Cs matrix were a hindrance due to the bulky structure of BTC filler. Therefore, the NH_2 groups of Cs matrix did not fully form a cationic side in the acidic medium, consequently reducing the percentage forming the hydrogen bonds and electrostatic interaction between the biocomposite components. In particular, the biocomposite films with 14 wt/v% of BTC filler were too brittle to be measured in tensile testing.

Figure 5 shows that ε_R values of the biocomposites decreased significantly with the addition of BTC filler from 2 to 10 wt/v%, but this reduction is still within an acceptable range. Meanwhile, the ε_R values of biocomposites with 10 wt/v% BTC filler loading are much lower than those with 0 wt/v% BTC filler loading, because the energy to cause the composite failure was smaller and stored in the composite material prior to failure as elastic strain energy.[63] At this point, the biocomposite films were considered to deform by local yielding and necking as suggested by the stress versus strain curves. Therefore, it can be claimed that the reduction of ε_R values was related to the ductility of the produced biocomposites. Two different types of chitosan were present in the biocomposites: crosslinked chitosan (BTC filler) and linear chitosan (Cs matrix). Generally, the ductility of a material tends to decrease in crosslinked structures.[64] Therefore, increasing the addition of BTC filler would reduce the ductility of the biocomposite. Its tendency toward ductility is decreased, as usual, with a resultant decrease in strain cracking and finally the reduction of ε_R values.

Additionally, the flexibility of polymer chains in the biocomposite network also affect ε_R values.[65] BTC filler was considered as rigid filler due to the stearic hindrance produced by the benzene ring on its structure. Generally, the structure of stearic hindrance would reduce the degree of flexibility of the polymer networks. In the other words, BTC provides the rigid constraints that limit the deformation of elastic elements in the biocomposites. Therefore, the stress over strain curves of the biocomposites shows roughly linear-elastic behavior to fracture. This trend is indicated by stress over stains curves with higher BTC filler loading. Contrarily, in the case of the biocomposites with 0 wt/v% of BTC filler loading, the flexibility of the film was considered stable due to the relatively higher Cs matrix content. Generally, chitosan polymer has a highly entangled polymer network with a high sliding friction between the polymer chains.[66] However, the chitosan polymer chains become somewhat uncoiled and separated in the presence of the BTC filler. At the excess levels of BTC filler loading (12 to 14 wt/v%), this phenomenon became increasingly notable. At this composition, the ε_R values decreased significantly, probably due to the discontinuity of Cs phases. The interconnectivity of the Cs matrix was limited and the BTC filler presented a hindrance. The superior ability to absorb energy under deformation could not be effectively provided by the Cs matrix. Therefore, the sliding properties of the chitosan polymer chains in the Cs matrix are considered to have been reduced by the presence of the BTC filler.

The E values of biocomposites increased dramatically with the addition of 2 to 10 wt/v% of BTC

filler. The increment can be explained by the extensibility and flexibility of the produced biocomposites. In the other words, at this composition of BTC filler, the biocomposite film was able to retain its loaf properties by maintaining its spatial expansion after the subjected force (load) was applied and during the relaxation of the BTC filler. Introduction of load causes intermingling, not only in the Cs matrix but also in the BTC filler. At this point, the energy stored in the rigidity of the BTC filler can only be released if the slip stick behavior allows it.[67] The slip stick behavior is positively correlated with the flexibility of the interfacial area of Cs matrix and BTC filler. Generally, the sample with greater flexibility properties is recognized to have better slip stick behavior. In the case of the produced biocomposites, optimum adjustment of the BTC filler slip stick behavior, either within the BTC filler or at the interface with the Cs matrix, is achieved through the crosslinking structure of the BTC filler. The crosslinked structure improved the recovery of BTC filler in introducing of load and consequently increased the loaf properties of the biocomposite film.

Another factor that contributed to the increment in E value was the geometry of the filler used in the biocomposites. The quality of interfacial bonding between Cs matrix and BTC filler depends primarily on the surface topography of the filler used since the topography of the filler material governs the way in which the stress is transferred between the biocomposite components.[68] The topography of the BTC filler was considered small and uniform in its size (50 to 80 μm). Therefore, the probability of small nicks and scratches on the surface of the BTC filler is reduced with the size of filler. The elasticity of the biocomposite material was increased by the smooth topography surface of BTC filler. Under the applied forces, a high energy at small deformation purposely to recover the elastic behavior of the biocomposites was needed with the smooth surface of BTC filler.

Furthermore, the E values of the biocomposite decreased at BTC filler loading of 12 and 14 wt/v%. However, the reduction values still remained higher than that of the biocomposite with 0 wt/v% of BTC filler loading. At this composition, the biocomposite tend to be stiff and rigid material with lower level of flexibility. Therefore, the reduction could be associated to the limited stretching behavior of the biocomposite under the applied force. Meanwhile, the orientation and distribution of BTC filler at the excess amount had also contributed to the reduction of E values.[69] Due to agglomeration of BTC filler, producing more homogenous distribution in Cs matrix become difficult. Consequently the BTC filler would form bundles of interaction between their components. At this point, the rigidity properties of BTC filler significantly increased. The rigid constrain that was provided by the bundles of BTC filler limit the deformation of elastic elements in the biocomposites.

An examination of the area under stress versus strain curves showed a toughness level of biocomposites film. In engineering definition, toughness is the work or energy stored by the deformed sample.[70] The most commonly used unit of work is J (Nm) or in/Ib. Generally, the stress versus strain curve of examined biocomposites tends to form instantaneous deformation characters with the addition of BTC filler. Addition of BTC filler over the range of examined composition into Cs matrix did not give significant effect to the K values of biocomposites. As a whole tendency, BTC filler is able to delocalize the strain out of the area of largest stress and consequently maintains the volume of the deformation biocomposites film. The delocalization is induced by weakening the biocomposites structure that perpendicular to the loading direction yielding a multiple cracking mechanism. At this point, the homogeneity and compatibility of BTC filler into Cs matrix are favorable in maintaining the K values of produced biocomposites film.

Tearing test

The tearing test was carried out to define the average gram force required to tear a single sheet of biocomposites film. Normally, the adequate amount of energy is required to expend the tearing process, since the tearing occurs when the stress (supplied by the tearing force) due to the indenter exceeds the strength of the material.

Figures 6 and 7 show the effect of BTC filler loading (0 to 14 wt/v%), towards tearing resistance of the biocomposites film. Generally, the load (F) versus displacement (DD) curves that are obtained for 0 to 4 wt/v% of BTC filler loading are geometrically similar to one another. The curves demonstrate that D shaped biocomposite film fail in a ductile manner after exhibiting a clear yield point and a drop in load after yield of deformation due to the separation process of the biocomposites film. This phenomenon was obviously noted for the biocomposites film with the lesser amount of BTC filler. However, the failure of the biocomposites with 6 to 10 wt/v% under tearing mode was progressively and directly taking part at the maximum F values. This type of failure was considered to occur after crack tip yielding.[71] Therefore, no deformation behavior was clearly observed on the F versus D curves. Furthermore, the loading level of BTC filler (wt/v%) had a profound effect on tearing properties of the biocomposites films. Figure 7 shows that values of F increase (≈33 to 50%) with the increasing of 2 to 10 wt/v% of BTC filler, respectively. However, the obtained D values decreased

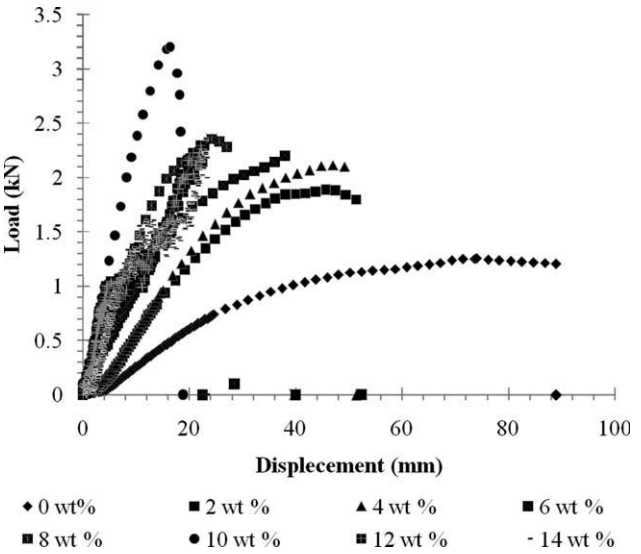

Figure 6 Tearing profile of the biocomposites over the range of BTC filler loading; (a) 0 wt/v%; (b) 2 wt/v%; (c) 4 wt/v%; (d) 6 wt/v%; (e) 8 wt/v%; (f) 10 wt/v%; (g) 12 wt/v%; and (h) 14 wt/v%.

sharply from 89 mm (for the biocomposites with 0 wt/v%) to 18.5 mm (for the biocomposites with 10 wt/v%). From the initial slope and maximum F values of the curves, values of Young's Modulus (E) were calculated. As expected, the E values of 2 to 10 wt/v% of BTC filler increased almost 30% with the increasing of BTC filler. Meanwhile, the E value obtained via the biocomposites with 10 wt/v% of BTC filler loading was 50% higher than the 0 wt/v% of BTC filler loading. As the E values increased, the biocomposites film tend to become more brittle and stronger (Fig. 6). The obtained tearing results can be explained by two main reasons.

First, the reinforcement of Cs matrix by virtue of homogenously dispersed BTC filler. The homogeneity would ensure a strong interaction between BTC filler and Cs matrix to take place. Thus, BTC filler would act as network fulcrum points in the biocomposites system to transfer the introduced tearing forces evenly to all other Cs chains (in Cs matrix). This in a general sense, enhances the tearing resist-

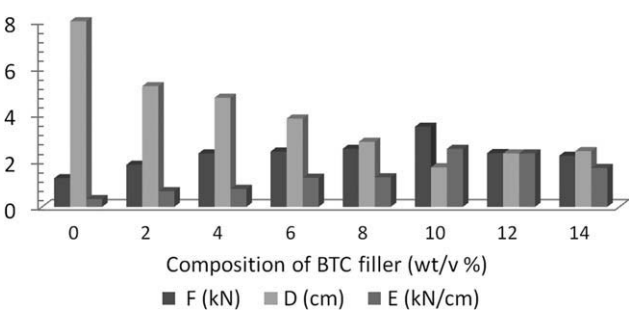

Figure 7 Variation of load (F); Displacement (mm) and Young's Modulus (E) of the BTC filled chitosan biocomposites at various percentage of BTC filler loading.

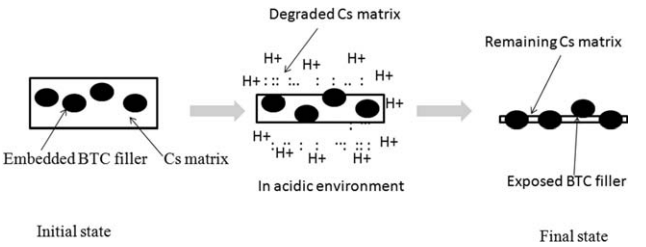

Figure 8 Mechanism of acid digestion process.

ance of the biocomposites. In other words, addition of the BTC filler resulted in producing a stiffer biocomposites film. Therefore, the tearing load is principally borne by the stiffness of the BTC filler up to yield point beyond which the stress of tearing transferred to the Cs matrix. Secondly, the BTC fillers are able to physically knot and tangle with the polymer chains of the Cs matrix since both of the components are chemically similar in polymer back-bone.[72] Therefore, the BTC filler is expected to have a well dispersion in the Cs matrix and the polymer networks of the biocomposites are linked by hydrogen bonds and electrostatic interaction. However, because the Cs polymer chains are strongly adhered to the interfacial region (between BTC filler and Cs matrix), thus the mobility of the polymer chain is significantly reduced. This probably increases the F and E values and decreases the D values of the biocomposites through the addition of BTC filler. Consequently, the substantial increase in tearing strength (via F and E values) is desirable in many membrane and packaging applications.

However, addition of BTC filler loading up to 12 and 14 wt/v% had given negative results on tearing properties of the biocomposites film (Figs. 6 and 7). The recorded F values dropped significantly (13 to 21%) from the biocomposites with 10 wt/v% of BTC filler loading. Meanwhile, insignificant changes were recorded for the D and E values with similar composition of the biocomposites. At this point, the mode of failure involved in the biocomposites films at the composition of 12 to 14 wt/v% was a crushing failure. The crushing failure described as a pattern in which the crushed films near the end line in a plane approximately parallel to the end surface.[73] In other words, the biocomposites at this level of BTC filler loading appeared to be notch sensitive material. Therefore, the structural elasticity of the biocomposites film was suppressed and consequently, the biocomposites exhibited a single point of failure. This phenomenon was associated to the poor interfacial bonding of the biocomposites components.[74] At this point, the present of BTC filler leads to lower inter particular distance of the composites. Because of this poor interfacial bonding, BTC filler would slip in the Cs matrix and automatically produced the failure mechanism of the whole structure of the biocomposites.

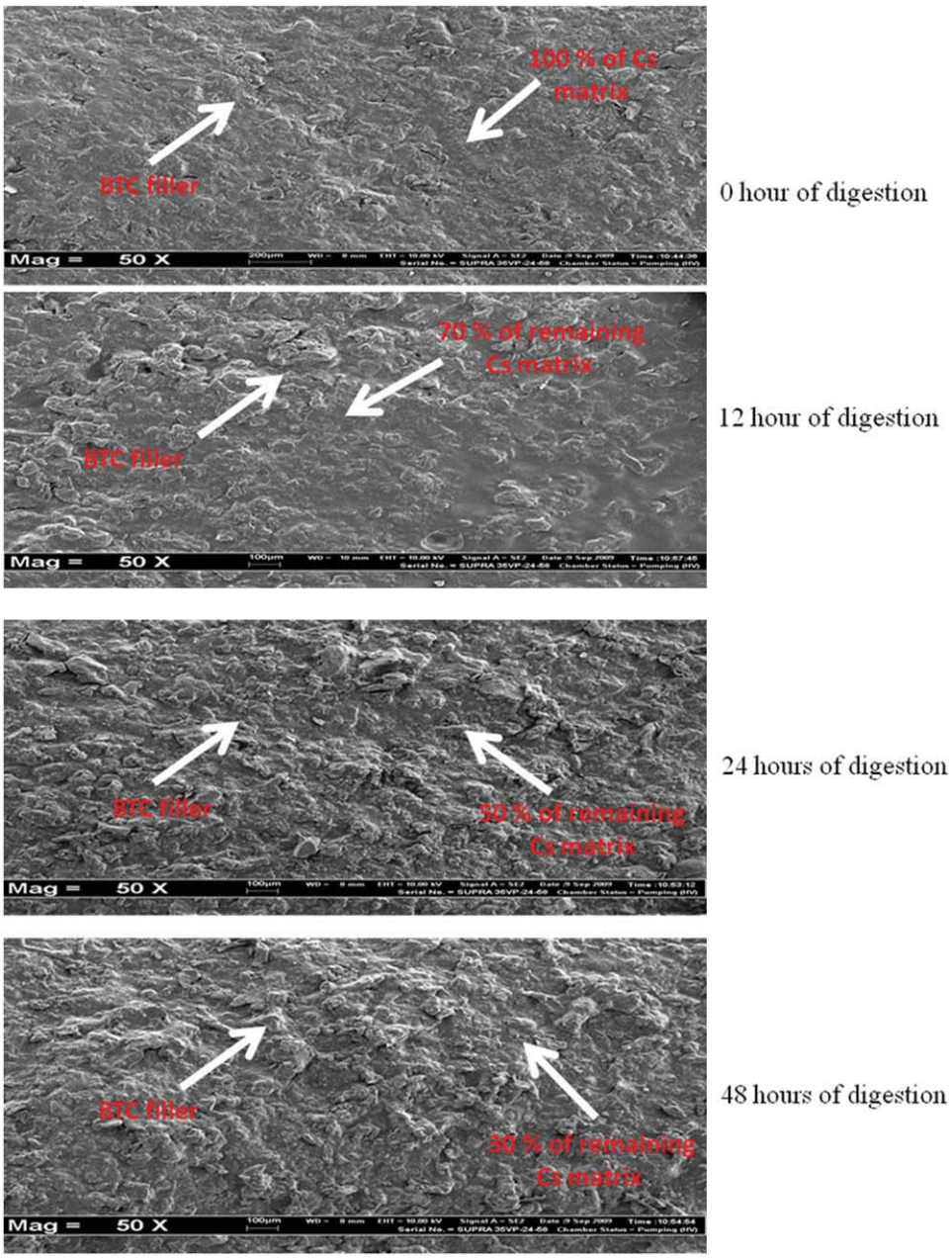

Figure 9 Acid digestion profiles of different soaking time (0; 12; 24 and 48 h). The images were taken at magnification of 50 X. The BTC filler distribution and Cs matrix were indicated by the errors. [Color figure can be viewed in the online issue, which is available at wileyonlinelibrary.com.]

The agreements of tensile and tearing results indicated that addition of BTC filler at certain level would produce Cs bio composites with better mechanical properties.

FESEM analysis

Characterization of BTC filler distribution

Filler distribution is the main factor that influenced the major properties of produced composite materials especially the mechanical properties. In this study, new approach named as "acid digestion process" has been investigated to effectively observed and study the distribution of BTC filler in Cs matrix. Similar approach can be applied in other Cs based biocomposites material. In this approach, a part of Cs matrix (≈70%) was progressively and robustly degraded in acid medium (0.1*M* acetic acid). As reported previously, the primary amine (NH_2) groups of chitosan polymer (that only present in Cs matrix) tend to form a polycationic species and

dissolved in acid medium due to the protonization process. The protonization process was carried out according to the above mechanism.

$$R - NH_2 + H^+ \rightleftharpoons R - NH_3^+$$

In this condition, the BTC filler was fully protected from being degraded in acidic medium due to its crosslinked structure and lack of reactive of the protonization side (NH-R). Therefore, the BTC filler would become the main remaining component that was present in the biocomposites system even after the acid digestion process. This process will finally leave the biocomposites material with the minimum thickness of Cs matrix without coated BTC filler. The minimum remaining content of Cs matrix was determined on the duration of soaking process (in acidic medium). However, the minimum thickness of Cs matrix was purposely needed to hold the BTC filler arrangement. At this point, the arrangement and distribution of BTC filler was clearly observed since the Cs matrix as the coating materials of BTC filler was completely removed. The mechanism of acid digestion process is fully illustrated in Figure 8.

Consequently, the FESEM analysis was applied to investigate the BTC distribution on the removal surface. The microscopic examination of the removal surface for 10 wt/v% of BTC filled Cs matrix at certain digestion of time (12 h; 24 h; and 48 h) are shown in Figure 9, respectively. The analysis was done using biocomposites with 10 wt/v% of BTC filler loading, since the biocomposites show the optimum and maximum in mechanical properties (with respect to the optimum values of σ_K and E) over all the composition of produced bi-composites.

In 12 and 24 h of acid digestion, the presence of BTC filler distribution and arrangement was doubted and limited to observe under FESEM analysis. At this point, the BTC filler was hindered and fully covered by the Cs matrix with 70 to 50% of BTC filler. However, the microscopic image produced by the biocomposites film exposed in acidic medium for 48 h, revealed a greater, homogenous and unity dispersion of BTC filler in Cs matrix. The FESEM image shows that the BTC filler was in the form of single particle indicating that the BTC filler had been separated effectively during the mixing process of sample preparation and as a result a well dispersion of BTC filler in Cs matrix. Good dispersion of single particle of BTC filler is expected in resulting very promising mechanical properties as been previously discussed in details. Besides, the BTC filler was strongly and perfectly lodged themselves at the interface between the phases of Cs matrix and consequently the stress transfer ability (from Cs matrix to BTC filler) of the biocomposites increased significantly. Meanwhile, the interfacial adhesion strength of BTC filler to Cs matrix was considered excellent since none of BTC filler was pulled out during the acid digestion process. During the stress transfer process, Cs polymer chains became stiff and rigid, making the biocomposite material less susceptible to stretching mechanism. Therefore, the enhancement in the mechanical properties of the biocomposites had shown clear results due to the addition of BTC filler into Cs matrix.

Fracture surface created from tensile test

To determine the cause of failure of produced biocomposites film, the fractured surface (under tension mode) of biocomposites film was analyzed by FESEM. Meanwhile, the FESEM approach was also carried out to indicate the directions in which cracks had grown and the locations of the final propagations. The selected micrographs that were taken from the fractured surfaces of the biocomposites films under tensile test is presented in Figure 10.

Generally, the micrograph images of biocomposites with 0 wt/v% of BTC filler (Fig. 10) show a homogenous plastic deformation behavior with slit-shaped and linear (unbranched) crack formation. Therefore, the majority of presented breaking surface clearly formed the parallel crack lines and largely perpendicular to the direction of the applied stress, since no permanent deformation was taken into account during the tensile test (Fig. 10). However, there was very little constraint or insignificant amount of contraction before the failure of the biocomposites had taken place. In other words, the fracture surface of biocomposites film with 0 wt/v% of BTC filler was relatively smooth by performing a ductile fracture micrograph.

Meanwhile, the microscopic observations demonstrated that at higher BTC filler loading (2 to 10 wt/v%), the crack propagation mechanism occurred progressively. The micrograph indicated that, at this range of BTC filler loading, the interfacial adhesive strength was sufficient to transfer the subjected load until failure initiated in the BTC filler, as evident by the presence some amount of Cs matrix between the BTC filler. Cracks extensions began macroscopically flat but was immediately accompanied by small "shear lips" at the side surfaces especially around the nearest area of main crack.[64] Propagation of the crack began because the decreased stored elastic energy of the biocomposite system became available and was greater than the energy necessary to create two new crack surfaces. As the crack extended, the shear lips widen and consequently covered the entire fractured surface which finally became fully slanted either as single or double shear. In short, three types of obvious cracks considered performing in the fractured surface of

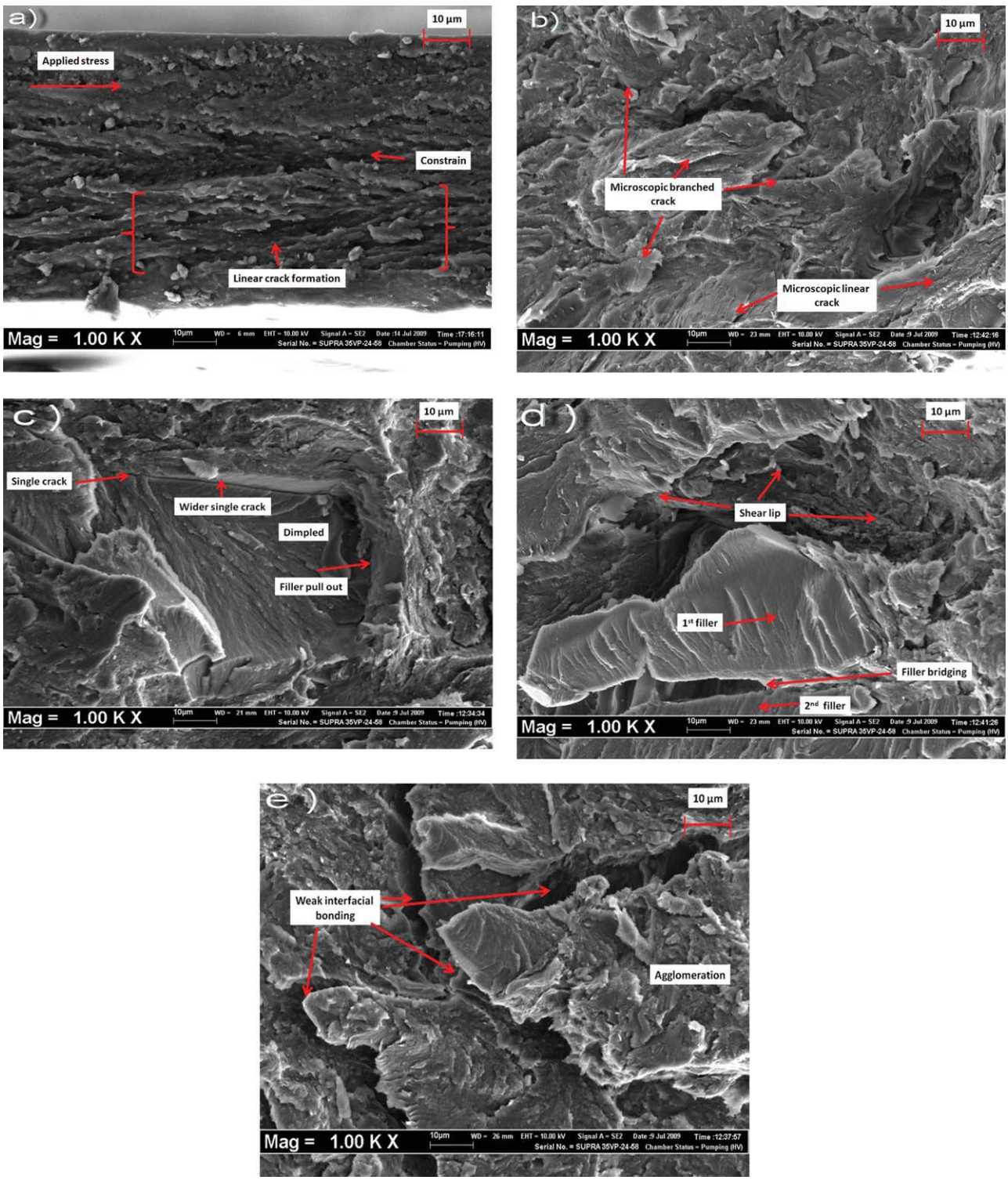

Figure 10 The series micrograph image (FESEM analysis) of fracture surface (under tensile test) of biocomposites at different of BTC filler loading [(a) 0 wt/v%; (b) 2 wt/v%; (c) 6 wt/v%; (d) 10 wt/v%; and (e) 12 wt/v%]. The images were analyzed under magnification of 1000×. [Color figure can be viewed in the online issue, which is available at wileyonlinelibrary.com.]

biocomposites due to this phenomenon which are; microscopic crack branching, kinking, and macroscopic crack branching. The macro branching cracks took place as the microscopic crack branching form outrun to others. The main mechanisms of micro branching crack that can occur during the tensile test in the biocomposites materials constitute of three different mechanisms; pull out, filler bridging

and debonding. During the pull out mechanism, the BTC filler is snapped from Cs matrix, generally after crack propagation. Moreover, with the BTC bridging mechanism, the interaction between BTC filler and Cs matrix are intense. However, as the pull out mechanism is active, not all the BTC filler are pulling out and broken; some remain and form a bridge between the parts of the fractured matrix. The pulled out BTC filler would leave an area named as "dimpled." Most of the performed dimples were equiaxed and encircling in shape since the fractured surface was obtained under unixial tensile loading test. Meanwhile, these bridging BTC filler make it difficult for the initial crack to spread and consequently increase the σ_K values of the biocomposite films. Debonding is characterized by the displacement between BTC filler and Cs matrix due to the present of an interface involving weak interaction. These mechanisms leads to the breaking of inter and intra hydrogen bonds that are present among the components of the biocomposites. Stress concentrations can lead to BTC filler failure or even to Cs matrix failure.

The mentioned crack phenomenon starts to occur as elastic energy is adequate to overcome the energy that is necessary to propagate a crack. The stresses at the apex of an elastic crack must have sufficient magnitude and capable of driving the crack to failure. The growth of each crack within the biocomposites system consumes energy (provided by the forcing mechanism of tensile test) from the available energy and creates new cracks surface. In the case of biocomposites, the presence of filler as reinforcement materials in Cs matrix limits the propagation of the crack.

Therefore, it is clearly observed that, the formation of micro crack in the fracture surface of biocomposites film with 2 to 10 wt/v% BTC filler loading having length much smaller than the crack present in biocomposites film with 0 wt/v% of BTC filler loading which indicated that greater amount of force (stress) is needed before the materials to be fail. In this situation, BTC filler with rigid properties acted as energy absorbent and increased the fracture energy of the biocomposites system by generating the smallest cracks (graze) through the BTC filler.

However, at the highest content BTC filler (12 and 14 wt/v%) bigger dimpled (due to the filler pull out mechanism) appearance on fractured surfaces became more significant and obviously observed. At this point, the interfacial bonds of Cs matrix and BTC filler was considered weaker due to the agglomeration of BTC filler in biocomposite system. Adhesion between the Cs matrix and BTC filler may be difficult with the agglomeration of the BTC filler, which can produce cracks that in turn may reduce σ_R values of biocomposite. At this point, the agglomerated BTC filler itself can be the crack initiator of the biocomposites. Consequently, the interfacial de-bonding would progressively take place. The biocomposites survive the breaking and bridge the cracks, giving rise in the de-bonding mechanism along the BTC filler and in the end a possibly local strain hardening. Therefore, the dimples appearance was seriously observed at this composition of the BTC filler loading. The arrow on the Figure 10 indicates that BTC filler and the dimples left by the filler after tensile test. The image show an agreement with the tensile test analysis which claimed that, at 12 to 14 wt/v% of BTC filler loading, the bonding between Cs matrix and BTC filler is considered weak and resulted in reduction of σ_R and E values.

Therefore, as the applied force (stress) increased in magnitude, micro crack continued to grow within the Cs matrix, and entered progressively into the BTC filler until their propagation were halted at almost BTC filler boundaries.

Fracture surface created from tearing test

The fracture morphology of the biocomposites was well corroborated by its tearing property since, the FESEM images show clear cut distinction between different tearing surfaces according to each composition of produced biocomposites film. The biocomposites with 0 wt/v% of BTC filler showed smooth and compact tearing micrographs. The crack propagation profiles shown were perpendicular to the tearing forces as indicated by the error (Fig. 11).

Meanwhile, FESEM analysis of biocomposites film with 2 to 10 wt/v% BTC filler (Fig. 11) revealed failure of the samples (under tearing mode) occurs after a series of sequential events. In other words, the breaking stretch of tearing fracture was obviously observed as the tearing testing was completed. The series of mechanism that are associated with the tearing process of the biocomposites films were identified as, opening and blunting of the initial crack tips (located in the middle of D-shaped dimension of samples); formation and propagation of a plastic deformation zone at each crack tip that originated from the main crack; overlapping the two plastic deformation zone with simultaneous major crack initiation (associated to the BTC filler pull out) and the final separation of the test specimen.

At this point, the biocomposites with 2 to 10 wt/v% of BTC filler loading was considered to have a better tearing adsorption as compared to other composition. There was lack of barrier between BT filler and Cs matrix. Additionally, under the FESEM analysis, the air hole structures were not significantly observed at the tearing fracture surface. Meanwhile, most of the BTC filler were broken at the same broken surface of the Cs matrix. At this point, the

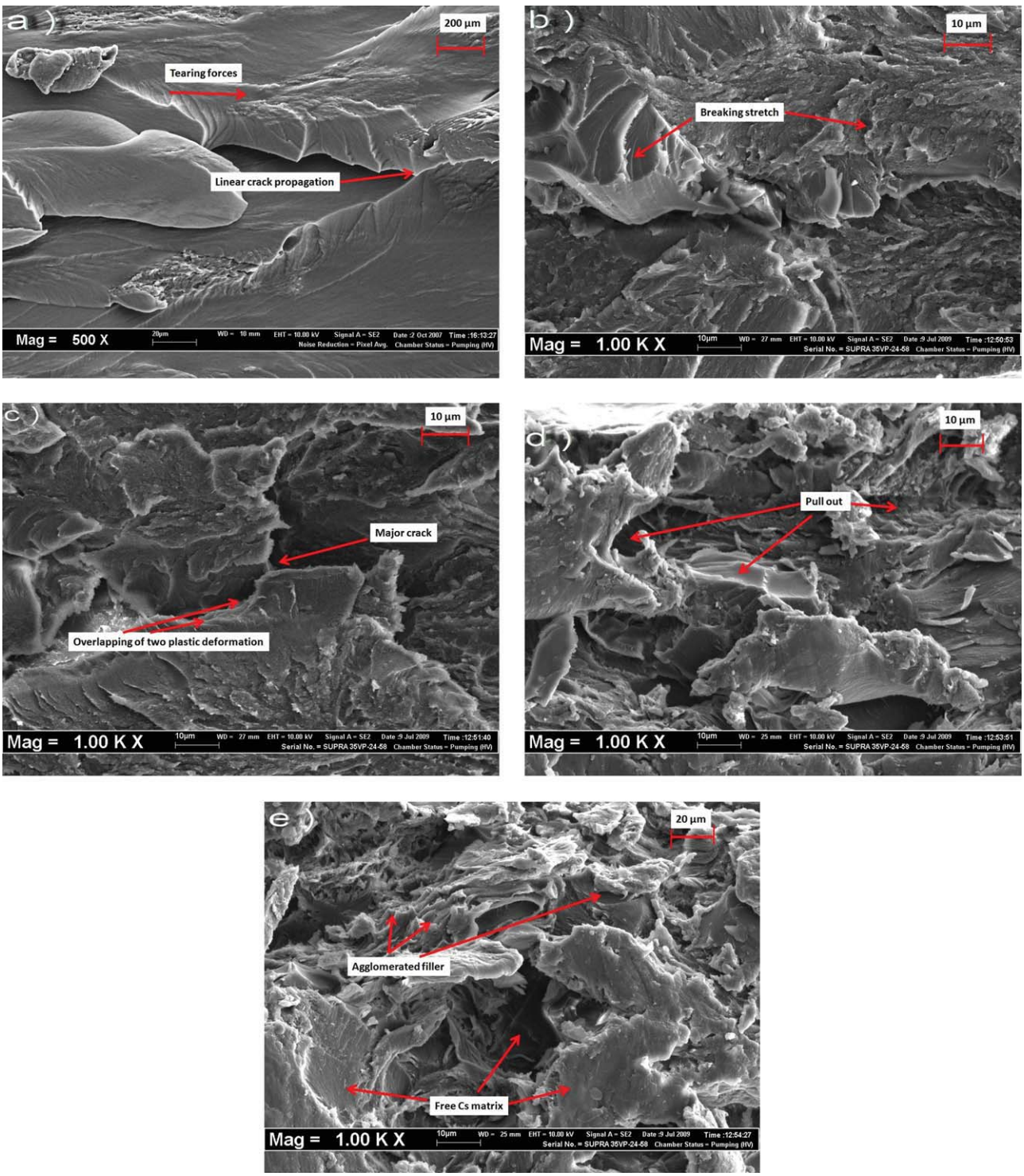

Figure 11 The series micrograph image (FESEM analysis) of fracture surface (under tearing test) of biocomposites at different of BTC filler [(a) 0 wt/v%; (b) 2 wt/v%; (c) 6 wt/v%; (d) 10 wt/v%; and (e) 12 wt/v%]. The images were analyzed under magnification of 1000×. [Color figure can be viewed in the online issue, which is available at wileyonlinelibrary.com.]

Cs matrix and BTC filler are assumed to have the same strain during the tearing deformation which BTC filler restricted the motion of Cs matrix.[75] In the case of biocomposites with higher amount of BTC filler (8 to 10 wt/v%), the Cs matrix and BTC filler broke at different strains. Some of the BTC filler was continuously broken after the Cs matrix was fully ruined. The BTC filler was pulled out and continued to elongate until failure mechanism occurred. These mentioned phenomena, indicated that the BTC filler and Cs matrix have a promising interfacial bonding, since both of components were hydrophilic.

As the addition of BTC filler increased to 12 and 14 wt/v%, abrupt change in the bonding quality had taken place. At this point, both of the BTC filler and Cs matrix broke simultaneously with the biocomposites failure strain probably due to the agglomeration of BTC filler. The cracks that were produced by the tearing forces were probably exacerbated by the presence of larger BTC filler in the as agglomerated particles that acted as defect nucleation and crack initiation sites.

CONCLUSIONS

The novelty of this study was associated to the crosslink's structure of the Cs biocomposites film. In this investigation, the crosslinks structure was mainly classified into two types, that is chemical and physical crosslinks. The first one was covalently bridge, which contributed by the structure of BTC filler and the electrostatic interaction while the second was hydrogen bonds that had taken place between BTC filler and Cs matrix. Through both interactions, the following conclusion was drawn:

1. A homogenous and well dispersed of biocomposites film forming mixture was successfully obtained as been confirmed by the chemical structure and acid digestion analysis (under FTIR and FESEM analysis), respectively.
2. The increment on mechanical properties of the biocomposites film was clearly observed through tensile and tearing test. The biocomposites with 2 to 10 wt/v% of BTC filler content had shown a similar trend of tensile and tearing results: increasing the content of BTC filler loading (wt/v%) led to increase in mechanical resistance (improvement of σ_R, F and E values) and decrease in elasticity and extensibility (reduction of ε_R and D values). However, the incorporation of 12 to 14 wt/v% of BTC filler in Cs matrix deteriorated the mentioned mechanical properties of the produced biocomposites.
3. The morphology image from FESEM analysis evidently demonstrates that as Cs matrix is reinforced with different amount of BTC filler, the morphology change on fracture surface of the biocomposite film is depending upon the interfacial interaction between the varying loading of BTC filler.
4. It was suggested that the promising mechanical properties of BTC filled chitosan biocomposites lend their potential application in thermal and sound insulation as well as in packaging and coating.

Appreciations are given to Fundamental Research Grant Scheme (FRGS) under Ministry of Science, Technology and Innovative (MOSTI) for funding this research works. N. M. Julkapli acknowledges the National Science Fellowship (NSF) under Ministry of Science, Technology and Innovative (MOSTI) Malaysia for the scholarship.

References

1. Rosa, D. S.; Grillo, D.; Bardi, M. A. G.; Calil, M. R.; Guedes, C. G. F.; Ramires, E. C.; Frollini, E. Polym Test 2008, 28, 842.
2. Panda, A. K.; Sigh, R. K.; Mishra, D. K. Renew Sust Energ Rev 2010, 14, 233.
3. Sriromreon, P.; Opaprakasit, M.; Petchsuk, A.; Opaprakasit, P. Adv Mat Resc 2008, 57, 789.
4. Anand, R.; Ramanujam, J. R.; Kulothungan, S.; Sharanya, V.; Murugalakshimi, C. N.; Bhuvaneswari, K. J Inds Poll Cont 2008, 24, 129.
5. Hakkarainen, M.; Albertsson, A. C. Adv Polym Sci 2008, 211, 85.
6. Shang, X. Y.; Fu, X.; Chen, X. D.; Yang, L. S. J App Polym Sci 2009, 114, 3574.
7. Mariani, P. D. S. C.; Allganer, K.; Oliveira, F. B.; Cardosa, E. J. B. N.; Innocentini-Mei, L. H. Polym Test 2009, 28, 824.
8. Chen, Y. D.; Pheng, J.; Liu, W. B. J App Polym Sci 2009, 113, 258.
9. Hofman, I.; Haas, D.; Eckert, A.; Ruf, H.; Firgo, H.; Muller, F. A.; Greil, P. Adv Appl Ceram 2008, 107, 293.
10. Ayuk, J. E.; Mathew, A. P.; Oksmanm, K. J App Polym Sci 2009, 114, 2723.
11. Tullo, A. H. Chem Eng News 2008, 86, 21.
12. Miranda, S. P.; Garnica, O.; Lara-Sagohan, V.; Cardenas, G. J Chil Chem Soc 2004, 49, 173.
13. Kai, C.; Ya, Z.; Xiao, H. W.; Qing, L. F.; Fu, Z. C. J Bioacte Comp Polym 2004, 19, 17.
14. Liuyun, J.; Yubao, L.; Li, Z.; Jianguo,, L. J Mater Sci 2008, 19, 987.
15. Walaikorn, N.; Nantana, J.; Sireerat, C.; Siriwan, K. Carbohyd Polym 2009, 78, 444.
16. Mahlous, M.; Tahtat, A. C.; Souza, B. S. W.; Cerqueira, M. A.; Teixeira, J. A.; Cruz, L.; Diaz, R.; Vicente, A. A. Food Hydrocolloid 2009, 23, 1895.
17. Xiadong, C.; Hua, D.; Chang, M. L.; Lucian, A. L. J App Polym Sci 2009, 113, 466.
18. Qian, L.; Jinping, Z.; Lina, Z. J Polymr Sci B 2009, 47, 1069.
19. Maria, V.; Ana, A.; Amparo, C.; Chelo, G. Food Hydrocolloid 2004, 23, 536.
20. Benamer, D.; Sundararajan, A. S.; Madihally, V. Biomaterials 2005, 26.5500.
21. Swapna, J. C.; Harish Prashanth, K. V. Rastogi, N. K.; Indiramma, A. R.; Reddy, S. Y.; Raghavaroa, M. S. Food Bioprocess Technol 2009, 203, 1.
22. Xu, Y. X.; Kim, K. M.; Hanna, M. A.; Nag, D. Inds Crops Prod 2005, 21, 185.
23. Jittrawadee, S.; Pitt, S.; John, B.; Ratana, R. Carbohyd Polymr 2005, 62, 130.
24. Garcia, M. A.; Pinottic, A.; Martino, M.; Zaritzky, N. Food Hydrocolloid 2009, 23, 722.
25. Anjali, D.; Smitha, B.; Sridhar, S.; Aminabhavi, T. M. 2005, 262, 91.
26. Julkapli, N. M.; Ahmad, Z.; Akil, H. M. e-polymer 2010, 077, 1.
27. Berger, J.; Reist, M.; Mayer, J. M.; Felt, O.; Peppas, N. A.; Gurny, R. Eur J Pharm Biopharm 2004, 57, 19.
28. Sionkowska, A.; Wisniewski, M.; Skopinska, J.; Kennedy, C. J.; Wess, T. J. Biomaterials 2004, 25, 795.
29. Rinaudo, M.; Pavlov, G.; Desbrieres, J. Polymer 1999, 40, 7029.
30. Melina, H.; Marie, C. H.; Andre, B. Int J Biol Macromol 2005, 37, 134.

31. Channasanon, S.; Graisuwan, W.; Kiatkamjornwong, S.; Hoven, V. P. J Colloid Interf Sci 2007, 316, 331.
32. Thacharodi, D.; Rao, K. P. Int J Pharm 1996, 134, 239.
33. Huang, R. Y. M.; Pal, R.; Moon, G. Y. J Membrane Sci 1999, 160, 17.
34. Margarita, D.; Montserrat, C.; Eduardo, R. H. Appl Clay Sci 2005, 28, 199.
35. Liu, C.; Bai, R. J Membrane Sci 2005, 267, 68.
36. Osman, Z.; Arof, A. K. Electrochim Acta 2003, 48, 993.
37. Chi, P.; Wang, J.; Liu, C. Mater Lett 2008, 62, 147.
38. Sun, H.; Lu, L.; Chen, X.; Jiang, Z. Sep Purif Technol 2008, 58, 429.
39. Paula, G.; Carlos, A. R. G.; Mary, K. S. B.; Luiz, F. P.; Paulo, A. P. S. Carbohyd Polym 2008, 71, 54.
40. Chad, D. B.; Lotte, K.; Masashi, N.; Ninus, C.; Dean, K. P.; Wayne, R. G.; Allan, S. H. J Control Release 2001, 72, 35.
41. Felinto, M. C. F. C.; Parra, D. F.; da Silva, C. C.; Angerami, J.; Oliveira, M. J. A.; Lugao, A. B. NIMPR B 2007, 265, 418.
42. Chen, J. H.; Liu, Q. L.; Fang, J.; Zhu, A. M.; Zhang, Q. G. J Colloid Interf Sci 2007, 316, 580.
43. Muzzarelli, C.; Stanic, V.; Gobbi, L.; Tosi, G, Muzzarelli, R. A. A. Carbohyd Polym 2004, 57, 73.
44. Enrique, J. B. Carbohyd Polym 2008, 74, 704.
45. Erol, A.; Osman, D. J Hazard Mater 2006, 136, 542.
46. Fernando, P.; Ernesto, G. Spectrochim Acta A 2000, 56, 2149.
47. Stefan, G.; Ulrike, T.; Iliyana, H.; Armin, L.; Richard, B.; Haspeter, H. Chem Phys Lett 2006, 421, 494.
48. Li, J.; He, Y.; Inoue, Y. J Polym Sci B 2001, 39, 2108.
49. Hashim, D. M.; Che Man, Y. B.; Norakasha, R.; Shuhaimi, M.; Salmah, Y.; Syahariza, Z. A. Food Chem 2010, 118, 856.
50. Md, S. S.; Soottawat, B.; Thummanoon, P. J Food Engng 2010, 96, 66.
51. Muzzarelli, A. A. R.; PieMorganti, P.; Morganti, G.; Palombo, P.; Palombo, M.; Biagini, G.; Belmonte, M. M.; Giantomassi, F.; Orlandi, F.; Muzzarelli, C. Carbohyd Polym 2007, 70, 274.
52. Du, D.; Chen, S.; Cai, J.; Song, D. J Electroanal Chem 2007, 611, 60.
53. Zhang, J.; Zhang, S.; Wang, Y.; Zeng, J. J Comp Mat 2007, 41, 1703.
54. Jiang, L.; Li, Y.; Wang, X.; Zhang, L.; Wen, J.; Gong, M. Carbohyd Polym 2008, 74, 680.
55. Muenduen, P.; Nirun, J. Carbohyd Polym 2008, 74, 482.
56. Booma, M.; Selke, S. E.; Giacin, J. R. J Elastmr Plast 1994, 26, 105.
57. Yen, M. T.; Yang, J. H.; Mau J. L. Carbohyd Polym 2008, 74, 840.
58. Zong, Z.; Kimura, Y.; Takahashi, M.; Yamane Y. Polymer 2000, 41, 899.
59. Hariraksapitak, P.; Supaphol, P.; J App Polym Sci 2010, 117, 3406.
60. Singha, A. S.; Thakur, V. K. Polym Plast Technol Engng 2009, 48, 736.
61. Munir, T.; Gulsoy, H. O. Int J Polym Mat 2008, 57, 258.
62. Han, E. H. M.; Leon, E. G. Prog Polym Sci 2005, 30, 915.
63. Lee, J. W.; Son, S. M.; Hong, S. I. J Food Eng 2008, 86, 484.
64. Annamalai, P. K.; Raj, P. S. Bioresource Technol 2008, 99, 8803.
65. Sailaja, R. R. N.; Girija, B.G.; Giridhar, M. J Mater Sci 2008, 43, 64.
66. Sanem, A. S.; Peter, K.; Martin, Y. L. Food Hydrocolloid 2009, 23, 202.
67. Wang, N.; Zhang, X.; Han, N.; Bai, S. Carbohyd Polym 2009, 76, 68.
68. Ramesh, S.; Tan, W.; Arof, A. K. Eur Polym J 2007, 43, 1963.
69. Mishra, S.; Naik, J. B. Polym Plast Technol 2005, 44, 511.
70. Lu, J.; Richard, P. W. Compos Sci Technol 2008, 68, 1025.
71. Heshemi, S. Polym Test 2003, 22, 589.
72. Maria, V.; Ana, A.; Amparo, C.; Chelo, G. M. Food Hydrocolloid 2009, 23, 536.
73. Tao, L.; Quan, C.; Linda, S. S.; Richard, W. S. Polym Compos 2002, 23, 1076.
74. Pauliukaite, R.; Ghica, M. E.; Fatibella-Filho, O.; Brett, C. M. A. Electrochim Acta 2010, 55, 6239.
75. Aparna, S.; Sundararajan, V. M. Biomaterials 2005, 26, 5500.